HHS Public Access

Author manuscript

Mol Cancer Ther. Author manuscript; available in PMC 2018 November 01.

Published in final edited form as:

Mol Cancer Ther. 2017 November ; 16(11): 2473–2485. doi:10.1158/1535-7163.MCT-16-0834.

Inhibition of discoidin domain receptor 1 reduces collagen-mediated tumorigenicity in pancreatic ductal adenocarcinoma

Kristina Y. Aguilera[1,%,^], **Huocong Huang**[1,%], **Wenting Du**[1], **Moriah M. Hagopian**[1], **Zhen Wang**[7], **Stefan Hinz**[1,#], **Tae Hyun Hwang**[2], **Huamin Wang**[5], **Jason B. Fleming**[6], **Diego H. Castrillon**[3], **Xiaomei Ren**[7], **Ke Ding**[7], and **Rolf A. Brekken**[1,4,*]

[1]Division of Surgical Oncology, Department of Surgery and Hamon Center for Therapeutic Oncology Research, UT Southwestern Medical Center, Dallas, Texas

[2]Department of Clinical Science, UT Southwestern Medical Center, Dallas, Texas

[3]Department of Pathology, UT Southwestern Medical Center, Dallas, Texas

[4]Department of Pharmacology, UT Southwestern Medical Center, Dallas, Texas

[5]Department of Pathology, UT MD Anderson Cancer Center, Houston, Texas

[6]Department of Surgical Oncology, UT MD Anderson Cancer Center, Houston, Texas

[7]School of Pharmacy, Jinan University, Guangzhou, China

Abstract

The extracellular matrix (ECM), a principal component of pancreatic ductal adenocarcinoma (PDA), is rich in fibrillar collagens that facilitate tumor cell survival and chemoresistance. Discoidin domain receptor 1 (DDR1) is a receptor tyrosine kinase that specifically binds fibrillar collagens and has been implicated in promoting cell proliferation, migration, adhesion, ECM remodeling, and response to growth factors. We found that collagen-induced activation of DDR1 stimulated pro-tumorigenic signaling through protein tyrosine kinase 2 (PYK2) and pseudopodium-enriched atypical kinase 1 (PEAK1) in pancreatic cancer cells. Pharmacologic inhibition of DDR1 with an ATP competitive orally available small molecule kinase inhibitor (7rh) abrogated collagen-induced DDR1 signaling in pancreatic tumor cells and consequently reduced colony formation and migration. Furthermore, the inhibition of DDR1 with 7rh showed striking efficacy in combination with chemotherapy in orthotopic xenografts and autochthonous pancreatic tumors where it significantly reduced DDR1 activation and downstream signaling, reduced primary tumor burden, and improved chemoresponse. These data demonstrate that targeting collagen-signaling in conjunction with conventional cytotoxic chemotherapy has the potential to improve outcome for pancreatic cancer patients.

[*]**Corresponding author**. Rolf A. Brekken, PhD, Hamon Center for Therapeutic Oncology Research, UT Southwestern Medical Center, 6000 Harry Hines Blvd., Dallas, TX 75390-8593, 214-648-5151, Rolf.Brekken@utsouthwestern.edu.

[%]equal contribution

[^]Current address: BerGenBio AS, Bergen, Norway

[#]Current address: University of Bergen, Bergen, Norway

Keywords

pancreatic cancer; DDR1; collagen; Peak1; 7rh; chemoresponse

Introduction

The extracellular matrix (ECM) is crucial for tumor progression. Specifically, the amount of ECM deposition correlates with a poor prognosis in cancer patients and ECM-mediated signaling can promote tumor cell survival and invasion (1–4). Fibrillar collagens, major components of tumor-associated ECM, signal through integrins and discoidin domain receptors (DDRs). The DDR family includes DDR1 and DDR2, which are closely related collagen-specific receptor tyrosine kinases (RTK) that recognize and bind several types of collagen (5–7). DDR1 and DDR2 are differentially expressed amongst tissue and cell types: DDR1 expression is predominant in epithelial cells and is found at high levels in the pancreas, brain, lung, kidney, spleen, and placenta (8–11), while DDR2 is found in cells of connective tissues that originate from embryonic mesoderm and is expressed highly in skeletal and heart muscle as well as kidney and lung (12–15). DDR1 and DDR2 are functionally important during development. For example, DDR1 participates in organogenesis and DDR2 is critical for bone development and growth (16). DDR1 and DDR2 contribute to key cellular processes, including cell migration, cell proliferation, cell differentiation, and cell survival (17).

Pancreatic ductal adenocarcinoma (PDA) has a collagen-rich microenvironment. Collagen is expressed in PDA by stromal cells, mainly fibroblasts, with a relatively minor but functionally-relevant contribution by tumor cells (18,19). Collagen receptors such as DDR1 have been linked in other tumor types to cellular processes that are prominent in PDA, including phenotypic plasticity (e.g., epithelial-to-mesenchymal transition [EMT]) and chemoresistance. For example, DDR1 can confer chemoresistance and mediate pro-survival signals in breast cancer and lymphoma cell lines (20,21) and may be involved in the recurrence of certain types of cancer (22). Further, Shintani et al. (23) found that collagen I induced N-cadherin expression (a marker of mesenchymal cells) in human pancreatic cancer cells required activation of DDR1. Moreover, the fact that DDR1 is expressed highly in a variety of tumor types suggests that this collagen-activated RTK may be involved in tumor progression (24–27). We establish here that activation of DDR1 contributes to the tumorigenic properties of PDA and that pharmacologically inhibiting this receptor tyrosine kinase with the selective DDR1 small molecule 7rh (28–31) slows tumor progression and enhances chemoresponse to standard-of-care PDA regimens.

Materials and methods

Cell lines

Human pancreatic cancer cell lines (AsPC-1, PANC-1, and BxPC-3) were purchased from the American Type Culture Collection (Manassas, VA) and were fingerprinted for validation of authenticity. The murine pancreatic cancer cell line Pan02 (also known as Panc02) was obtained from the NCI (DCTD Tumor Repository). Cells were cultured in DMEM

(Invitrogen) or RPMI (Invitrogen) containing 5% fetal bovine serum (FBS) and maintained at 37°C in a humidified incubator with 5% CO_2 and 95% air.

Wound healing (scratch) assay

Cells were cultured in 6-well tissue culture plates at high density (~90% confluence) in 2 ml of media with 5% FBS. Uniform scratches were made down the center of each well with a p20 pipette tip, cells were gently washed with PBS to remove the loose cell debris, and drug was added in media containing 5% FBS. 7rh was added in four 4-fold dilutions, to respective wells, and a DMSO control was added to respective wells to demonstrate the vehicle-independent effect. Cells were plated on respective culture conditions and images from the center of each well were taken at 0, 10, 20, and 30 hours. The wound width (μm) was measured using NIS Elements AR 2.30 software. The initial wound width was used to verify consistency in scratches.

Liquid colony forming assay

Cells were cultured in 6-well tissue culture plates at low density (250 cells per well) in 2 ml of media with 5% FBS with or without 7rh for approximately 1.5–2.0 weeks or until significant colony formation. 7rh was added in four 4-fold dilutions to respective wells, and a DMSO control was added to respective wells to demonstrate the vehicle-independent effect. Cells were then fixed with 10% formalin and stained with crystal violet. Images were analyzed with Image J.

Antibodies

Assays were performed with antibodies against: phospho-DDR1 (Tyr792, Cell Signaling #11994), DDR1 (D1G6, Cell Signaling #5583), phospho-SRC (Tyr416, Cell Signaling #2101), SRC (Cell Signaling #2108), phospho-PYK2 (Tyr402, Cell Signaling #3291), PYK2 (Cell Signaling #3292), α-Amylase (D55H10, Cell Signaling #3796), vimentin (Millipore AB5733), phospho-FAK (Abcam #4803), FAK (Cell Signaling #3285), PEAK1 (Millipore 09-274) phospho-PEAK1 (Tyr665, Millipore #ABT52), ϒH2AX (Ser139, Novus #NB100-384), and cleaved caspase-3 (Asp175, Cell Signaling #9661).

Western blot analysis

Sub-confluent monolayers of cells were lysed, supernatants were recovered by centrifugation at 13,000 rpm, protein concentration was measured, and equal amounts of total protein were separated by SDS-PAGE. Proteins were transferred to PVDF membranes (Bio-Rad; Hercules, CA) followed by blockade for 1 hour in 5% milk in TBS-T. The membranes were incubated overnight at 4°C with primary antibodies. Primary antibodies used are detailed above. Membranes were incubated with the corresponding HRP-conjugated secondary antibody (Pierce Biotechnologies; Rockford, IL) for 1 to 2 hours. Specific bands were detected using the enhanced chemiluminescence reagent (ECL, Perkin Elmer Life Sciences; Boston, MA) on autoradiographic film.

Immunoprecipitation

Cell lines were lysed in modified radioimmunoprecipitation assay buffer (0.5% deoxycholate, 0.5% SDS, 1% Triton X-100, 10 mM sodium phosphate, pH 7.2, 150 mM sodium chloride) with protease inhibitor (Complete Mini, Roche Life Science). Lysis was performed on serum-starved adherent cells after washing with chilled PBS. Lysates were allowed to rotate at 4°C on a nutator for 1 hour and then vortexed several times before centrifuging at 13,000 rpm for 10 min to pellet any insoluble material. Lysates were pre-cleared with protein A/G beads (Thermo Fisher Scientific). We used 200 μg cellular protein in 1 ml lysis buffer per immunoprecipitation reaction. To each sample, 1 μg of the appropriate antibody was added with 50 μl protein A/G bead slurry; each sample was then allowed to rotate overnight at 4°C on a nutator. Immunoprecipitated complexes were washed twice in lysis buffer, boiled in sample buffer, and subjected to SDS-PAGE and Western blot analysis.

siRNA-mediated knockdown of DDR1

Cells were plated 18–24 hours before transfection (1 × 10^5 cells/well in 6-well dish) at an initial confluence of 60%–80%. TransIT-siQUEST reagent and siRNA complexes were prepared and added according to manufacturer instructions (Mirus Bio, LLC). siRNA complexes were added to the cells at a final siRNA complex concentration of 1 μM. Protein was harvested 72 hours post transfection for Western blot analysis. siRNA duplexes were purchased from Integrated DNA Technologies. DDR1 duplexes used were (NM_001954 duplexes 1–3):

Duplex #1 = 5’-GUCUUGUAGCUAGAACUUCUCUAAG-3’,

3’-GUCAGAACAUCGAUCUUGAAGAGAUUC-5’;

Duplex #2: 5’-GCACUAGGCAGGUAAUAAUAAAGGT-3’,

3’ GACGUGAUCCGUCCAUUAUUAUUUCCA-5’;

Duplex #3: 5’-ACACUAAUAUAUGGACCUAGAUUGA-3’,

3’-AAUGUGAUUAUAUACCUGGAUCGAACU-5’.

Sircol collagen assay

Cell lines were prepared as indicated by the Sircol manual (Sircol Collagen Assay Kit, Oubis Ltd). Sircol dye reagent was used to saturate the collagen in the supernatant. The colorimetric principle of the Sircol collagen assay is the binding of a dye to collagen. A collagen-dye complex formed and precipitated out, was recovered by centrifugation, eluted with alkali, and measured with a spectrophotometer at 555 nm. The intensity of color measurement was proportional to the collagen concentration in the sample.

Animal studies

All animals were housed in a pathogen-free facility with access to food and water *ad libitum*. *C57BL/6* and *NOD-SCID* mice were purchased from the UT Southwestern Mouse Breeding Core. $Kras^{LSL\text{-}G12D/+}$; $Trp53^{LSL\text{-}R172H/+}$; $p48^{Cre/+}$ (*KPC*) mice were generated as previously described (32). Pan02 cells (5×10^5) were injected orthotopically in 6–8 week old *C57BL/6*

mice as described (33,34). Mice bearing orthotopic Pan02 tumors were used for multiple studies as indicated in Table 1. Eight week old *NOD SCID* mice were injected orthotopically with 1×10^6 AsPC-1 cells as described (33,34). Twenty-seven days after tumor cell injection mice were randomized to receive treatment as indicated in Table 1. Experiments were approved and performed in accordance with the Institutional Animal Care and Use Committee at UT Southwestern. For endpoint studies, experiments were stopped after the designated time post-tumor cell implantation. For survival studies, therapy was maintained until mice attained tumor-burden criteria (a loss of >15% body weight, significant reduction of activity, loss of strength, excessive ascites) requiring sacrifice. Plasma from *C57BL/6* mice bearing orthotopic Pan02 tumors was collected at the time of sacrifice. The plasma level of albumin, liver transaminases, aspartate transaminase, blood urea nitrogen, creatine, glucose, total bilirubin, and plasma total protein was evaluated by the Mouse Metabolic Phenotyping Core (UT Southwestern). For all therapy studies the person administering therapy was not blinded to the therapy groups. For survival studies, evaluation of health of the animals was determined by the person administering therapy and an independent observer, a decision to sacrifice the animals due to poor performance was determined by consultation between each investigator.

Histology and TMA sample analysis

Formalin-fixed tissues were embedded in paraffin and sectioned. Tissue samples from *in vivo* experiments were stained by Masson's Trichrome by the Molecular Pathology Core (UT Southwestern). Human (44) and matched PATX (150) TMA samples were scored on a scale of 0 (no stain) to 4 (very high stain) independently by two researchers, and the data were collected and plotted accordingly.

Statistical analysis

Fluorescent images were captured with a Photometric Coolsnap HQ camera using NIS Elements AR 2.3 Software (Nikon). Color images were obtained with a Nikon Eclipse E600 microscope using a Nikon Digital Dx1200me camera and ACT1 software (Universal Imaging Corporation). Pictures were analyzed using NIS Elements (Nikon). Quantification of immunohistochemistry was conducted using NIS Elements 3.2 software (Nikon Instruments). All data were analyzed using GraphPad Prism 5.0 software (GraphPad Software, Inc.). Datasets were analyzed by Student's t-test or ANOVA followed by Dunn post-test or Tukey's MCT, and results were considered as significant at $p < 0.05$. Results are shown as mean ± SEM.

Results

Association of DDR1 signaling with enhanced malignancy

To characterize the level of collagen-mediated DDR1 signaling in PDA, we determined the expression of phosphorylated DDR1 and phosphorylated PEAK1 in human pancreatic tumor samples with matched patient-derived tumor xenograft (PATX) samples. Primary tumors (44) and PATX samples (150) showed robust activation of DDR1 and PEAK1 (Figure 1a–c). The overall percentages of staining positivity are shown in Figure 1c. Furthermore, we examined the expression of active Ddr1, Pyk2, and Peak1, as well as the expression of Muc1

and Sox9 in pancreatic tumors from early (3 month) and later (5 month) stages of the *KPC (Kras$^{LSL-G12D/+}$; Trp53$^{LSL-R172H/+}$; p48$^{Cre/+}$)* mouse model of PDA (Figure 1d). The *KPC* model recapitulates many of the pathological features seen in human PDA including a dense stromal reaction (35) (Figure 1e–1f). Trichrome analysis revealed robust collagen deposition throughout PDA lesions in *KPC* mice (Figure 1f). Ddr1 activation and downstream signaling (Pyk2 and Peak1) were present in early pancreatic intraepithelial (PanIN) lesions as shown by correlative staining with a marker of early PDA lesions, Muc-1. Additionally, these effectors were expressed highly throughout the tumor epithelium at the later stage of the model (5month old *KPC*) as identified by areas expressing Sox9 (Figure 1d). Sox9 is expressed in the malignant epithelium and is confined to the duct-like cells; differentiated acinar and endocrine cells do not express Sox9 (36,37). These data demonstrate that collagen signaling via DDR1 is active in human PDA and mouse models of the disease.

Regulation of collagen signaling in PDA cell lines

The level of collagen expressed and secreted by AsPC-1 and PANC-1 cells was determined by a Sircol assay (Figure 2a). AsPC-1 cells expressed a higher level of secreted collagen than PANC-1 cells. The addition of exogenous soluble collagen enhanced the phosphorylation of DDR1, PEAK1, and PYK2 in AsPC-1, PANC-1, and BxPC-3 cells in a time-dependent manner. Consistent with other reports (38) we found that activation of DDR1 resulted in decreased expression of total DDR1 (Figure 2b). The downstream effectors of DDR1 are ill-defined (16,17); however, we found that phosphorylation of PYK2 and PEAK1 was induced by collagen robustly in AsPc-1 cells but less so in PANC-1 and BxPC-3 cells. Further, we found that Phosphorylated PYK2 and PEAK1, but not integrin αv co-immunoprecipitated with DDR1 from AsPC-1 cells (Figure 2c). To further define the contribution of DDR1 to collagen signaling, AsPC-1 cells were stimulated with collagen after siRNA-mediated knockdown of DDR1. Loss of DDR1 expression abrogated the activation of PEAK1 and SRC (Figure 2d–2e), as well as cell migration (Figure 2f). These data support the premise that collagen-mediated activation of DDR1 induces a signal pathway that includes PEAK1, SRC, and PYK2, which in turn are potentially responsible for collagen-induced chemoresistance (3,39) and tumor progression.

To demonstrate that DDR1 participates in chemoresponse in PDA, we evaluated the effect of the small molecule kinase inhibitor 3-(2-Pyrazolo[1,5-a]pyrimidin-6-yl)-ethynyl) 7rh benzamide (7rh) (28) on collagen-induced signaling in PANC-1 cells. The specificity of 7rh is high for DDR1 versus other related kinases (IC_{50}: DDR1, 6.8 nM; DDR2, 101.4 nM; Bcr-Abl, 355 nM) based on previously published cell-free kinase assays (28). In PANC-1 cells, 7rh inhibited DDR1-mediated signaling induced by soluble collagen (50 μg/ml) in a concentration-dependent manner (Figure 3a). At pharmacologically-relevant concentrations, 7rh inhibited activation of PYK2 and PEAK1, signaling proteins downstream of DDR1 (40). However, 7rh did not affect the activation of focal adhesion kinase (FAK), an effector that has not been previously associated with DDR1-induced signaling (23). Inhibition of the DDR1 signaling with 7rh also reduced cell migration (Figure 3b) and colony formation (Figure 3c) in a concentration-dependent manner.

7rh benzamide inhibits collagen-mediated signaling *in vivo*

Before initiating the *in vivo* studies, murine pancreatic (Pan02) cells were investigated for the effect of 7rh on collagen-induced Ddr1 signaling *in vitro* (Figure 4a), which demonstrated that 7rh inhibited Ddr1 activation in a dose-dependent manner. Prior pharmacokinetic studies (28) established the *in vivo* half-life of 7rh to be ~12 hours in rats. To determine an appropriate dose for therapy studies, mice bearing established orthotopic Pan02 pancreatic tumors were given a single dose of 0.1, 1, or 10 mg/kg of 7rh via oral gavage (Supplementary Figure 1). Tumor tissue was collected 12 hours post treatment and analyzed for Ddr1 activity. We found that 7rh at 1 mg/kg and 10 mg/kg significantly reduced the phosphorylation of Ddr1 as well as downstream effectors Pyk2 and Peak1, and resulted in an increased apoptotic index (cleaved caspase-3) (Supplementary Figure 1b–1e) as shown by immunohistochemical analysis. After demonstration that 7rh can reduce Ddr1 activity in the tumor microenvironment a single-agent therapy experiment was performed using a titration of 7rh for 2 weeks. Mice bearing established orthotopic Pan02 tumors were treated with 7rh (3, 10, or 30 mg/kg, 3×/week) via oral gavage (Supplementary Figure 2). 7rh at 10 mg/kg and 30 mg/kg resulted in an increase in normal pancreatic tissue as determined by H&E histology and expression of amylase, a marker of normal acinar tissue (Supplementary Figure 2b–2c). At these concentrations, 7rh also significantly reduced the level of phosphorylated Ddr1 and Peak1 (Supplementary Figure 2d–2e), increased apoptosis (Supplementary Figure 2f), as well as inhibited cell proliferation noted by the reduction of PCNA levels (Supplementary Figure 2g). These findings were corroborated by Western blot analysis of tumor lysates that showed a 7rh-dependent reduction of Peak1 phosphorylation (Supplementary Figure 2h). In addition, 7rh showed no apparent normal tissue toxicity as demonstrated by the maintenance of body weight and the lack of changes in plasma metabolites specific for liver and kidney function (Supplementary Figure 3a–3b). Metabolites analyzed included Alb (albumin), Alt (liver transaminases), Ast (aspartate transaminase), Bun (blood urea nitrogen), Crea (creatine), Glu (glucose), Tbil (total bilirubin), and Tp (plasma total protein). Next we performed a single-agent therapy experiment with a fixed concentration of 7rh. Mice bearing established orthotopic Pan02 tumors were treated with 7rh (25 mg/kg, 3×/week; Figure 4). Therapy was initiated 19 days post tumor cell injection and continued until experiment day 40, at which point animals were sacrificed (Figure 4b). We found that 7rh significantly reduced primary tumor weight (Figure 4c). Histological analysis of pancreata from these animals showed that 7rh slowed the progression of disease (Figure 4d). This is consistent with increased amylase expression (Figure 4e) and a significant decrease in Ddr1, Peak1, and Pyk2 activation (Figure 4f–4h) in animals receiving 7rh. This was concordant with enhanced apoptosis (cleaved caspase-3, Figure 4i) and reduced proliferation (PCNA, Figure 4j) in the presence of 7rh therapy.

To assess if 7rh enhanced the efficacy of chemotherapy *in vivo*, we combined 7rh with the standard-of-care chemotherapy of PDA (gemcitabine and nab-paclitaxel) in a xenograft model of PDA (Figure 5a). Immunocompromised animals bearing orthotopic AsPC-1 tumors were treated with vehicle, 7rh monotherapy (25 mg/kg, 3×/week), the standard-of-care regimen (chemo: gemcitabine, 15 mg/kg, 2×/week; nab-paclitaxel, 5 mg/kg, 2×/week), or the combination (combo) of 7rh and chemotherapy (Figure 5a). Therapy was initiated 27 days post tumor cell injection and 3 animals from each cohort were sacrificed on day 28

(one day post therapy induction) to document tumor burden at the start of therapy (initial group). Each regimen was continued until individual animals became moribund, at which point the moribund animals were sacrificed. The combination of 7rh + chemotherapy significantly enhanced the median overall survival to 98 days, compared to chemotherapy, 7rh, or vehicle at 73, 57, and 54.5 days, respectively. After the median survival was achieved for the combination group, therapy was withdrawn at day 102 to assess the consequence of therapy removal (withdrawn group; Figure 5b–5c, Supplementary Figure 4). Tumor tissue from each group was analyzed by histology and immunohistochemistry. Combination therapy resulted in more normal pancreatic tissue (H&E), a significant reduction in collagen signaling (P-DDR1, P-PYK2, P-PEAK1), a reduction in vimentin expression as well as cell proliferation (PCNA), and enhanced apoptosis (cleaved caspase-3) and DNA damage (γH2AX; Figure 5d–5k). Withdrawal of therapy from the combination group resulted in restoration of cell proliferation as well as vimentin expression and collagen signaling to levels similar to that observed in vehicle-treated animals. Additionally, we noted that 7rh alone or in combination with chemotherapy reduced trichrome staining, suggesting a reduction in fibrosis (Supplementary Figure 4a). Tumor weight vs. survival days was plotted (Supplementary Figure 4b) and indicated that therapy with 7rh, chemotherapy, or the combination reduced primary tumor growth compared to treatment with vehicle. Animal weight was monitored throughout the experiment and no therapy-induced changes in body weight were noted (Supplementary Figure 4c).

To determine if the therapeutic efficacy of 7rh combinatorial therapy extended to more rigorous *in vivo* models, we moved to a genetically engineered mouse model (GEMM) of PDA. *KPC (LSL-Kras$^{G12D/+}$; LSL-Trp53$^{R172H/+}$; p48$^{Cre/+}$)* mice were enrolled into therapy cohorts at 4 months of age (Figure 6), a time point we have found where greater than 90% of animals have established PDA. Treatment arms were the same as the AsPC-1 xenograft experiment and contained 12 animals/cohort. An additional 9 animals were sacrificed at the start of therapy to document mean tumor burden at the initiation of the experiment. The average tumor burden of these 9 animals was 0.27 g. Treatment with the combination regimen enhanced median of survival to 208 days compared to treatment with chemotherapy, 7rh, or vehicle at 180, 159, and 144 days respectively (Figure 6b–6c). Immunohistochemical analyses of tumor tissue harvested at the time of sacrifice demonstrated that inhibition of Ddr1 with 7rh suppressed collagen signaling (P-Ddr1 and P-Peak1), reduced vimentin expression and cell proliferation (PCNA) while increasing apoptosis (cleaved caspase-3) and DNA damage (γH2ax; Figure 6d–6j). Chemotherapy with gemcitabine and nab-paclitaxel also reduced collagen signaling and vimentin expression as well as decreased the number of PCNA-positive cells. Additionally, treatment with 7rh alone, chemotherapy alone, or the combination induced a reduction in trichrome staining (Supplementary Figure 5a). Tumor weight vs. survival days was plotted (Supplementary Figure 5b) and indicated that therapy with 7rh, conventional chemotherapy, or the combination reduced primary tumor growth compared to treatment with vehicle. Animal weight was not adversely affected by therapy (Supplementary Figure 5c). These data demonstrate that Ddr1 inhibition can increase the efficacy of standard-of-care chemotherapy in robust preclinical models of PDA.

Discussion

The goal of this project was to investigate the contribution of collagen-mediated DDR1 signaling to PDA progression. We demonstrated that DDR1 and downstream effectors are expressed and activated in human and mouse PDA. Additionally, we found that a novel small-molecule inhibitor, 7rh benzamide (28), effectively abrogated DDR1 signaling thereby reducing liquid colony tumor cell formation and tumor cell migration. Further, we found that 7rh inhibits its target and has significant therapeutic efficacy *in vivo* at doses that are free from observable tissue toxicity. Finally, 7rh significantly improved the efficacy of standard-of-care chemotherapy in robust mouse models of PDA. Overall these data highlight that collagen signaling through DDR1 is a critical and pharmacologically targetable pathway in PDA.

Physiological chemoresistance can result from the accumulation of ECM proteins in the tumor microenvironment, a common characteristic of PDA. The dysregulation of ECM-driven signaling can enhance the hostile programs of cancer cells (16). This fibrotic network contributes to the development of a complex tumor microenvironment that promotes PDA development, invasion, metastasis, and resistance to chemotherapy (41). However the ECM-mediated signaling pathways that drive these programs are unclear and the mechanisms of how collagen-mediated DDR1 signaling in particular affects tumor progression require additional investigation.

We previously found that the matricellular protein Sparc (secreted protein acidic and rich in cysteine) reduced collagen I signaling through Ddr1 and that loss of *Sparc* accelerated PDA progression with a concordant increase in Ddr1 signaling (42). Furthermore, prior reports on the expression of SPARC in pancreatic tumor cells demonstrated that there is a reduction in SPARC expression by promoter hypermethylation in a high frequency of pancreatic tumor cells and other epithelial cancer cells (43,44). Additionally, it was reported that the restoration of SPARC expression enhanced radiosensitivity and chemosensitivity in preclinical models of colon cancer (45) and that SPARC expression enhanced chemoresponse in cancer patients (46,47). Thus there was compelling evidence that the loss of tumor cell expression of SPARC correlated with tumor progression and poor chemoresponse. We propose that these observations can be explained by the fact that SPARC inhibits collagen-induced DDR1 activation. This is consistent with reports that collagen signaling is associated with chemoresistance in PDA cell lines (3,48) and that DDR1 confers resistance to chemotherapy and mediates pro-survival signals (20,21,49).

Our studies relied on syngeneic, xenograft, and genetic models of PDA. We chose to utilize Pan02 (also known as Panc02) cells because this cell line grows in *C57Bl/6* immunocompetent animals, a useful system to evaluate initial toxicity and efficacy of DDR1 inhibition with 7rh. We employed AsPC1 cells, a commonly used human PDA cell line, because these cells express high levels of endogenous DDR1 activation *in vitro* and grow robustly *in vivo*. We also used the *KPC* model of PDA, which incorporates two common genetic lesions present in human PDA (e.g., KRAS activation and *p53* loss). We believe this model is well-suited for endpoint and survival studies as mice develop advanced PDA with

100% penetrance at approximately 3–4 months of age and tumor progression recapitulates many of the characteristics of human PDA (35).

DDR1 is upregulated in fibrotic diseases and contributes to the initiation and progression of fibrosis (50). We observed reduced collagen deposition in tumors from mice treated with 7rh, thus the inhibition of DDR1 might improve response to chemotherapy in a cell autonomous manner and also improve drug delivery without disrupting the function of cancer-associated fibroblasts. DDR1 inhibition has also been shown to reduce tumorigenicity in multiple tumor models (23,25,51,52). For example, silencing DDR1 by siRNA has been shown to reduce metastatic activity in lung cancer models (27,51) and enhance chemosensitivity to genotoxic drugs in breast cancer cells (49). Additionally, we have recently reported that DDR1 expression and activity correlates with worse outcome in a cohort of gastric cancer patients (31). In this study, 7rh-mediated inhibition of DDR1 in gastric cancer cells reduced tumorigenic characteristics *in vitro* and tumor growth *in vivo*. Finally, collagen signaling and DDR1 activity has been linked to epithelial plasticity (23,40). We found evidence that 7rh induced a more differentiated tumor cell phenotype, which is consistent with improved efficacy of standard chemotherapy.

Several small molecule inhibitors (imatinib, nilotinib, and dasatinib) that target breakpoint cluster region-Abelson kinase (BCR-ABL) also potently inhibit DDR1/DDR2 activity (53,54). Thus, the potential activity of imatinib and vinorelbine in a phase I/II trial in metastatic breast cancer patients (55), as well as dasatinib in numerous clinical trials in solid tumors (56), could be due in part to the inhibition of DDRs. Dasatinib in particular has demonstrated promising therapeutic efficacy in lung cancer cells (57) and squamous cell carcinoma patients (58) harboring gain-of-function DDR2 mutations.

Our data suggest that the inhibition of DDR1 can improve the efficacy of standard chemotherapy for pancreatic cancer. Critical questions regarding the contribution of DDR1 to tumor progression remain, including whether the results we have found will extend to other solid tumors (e.g., lung, breast). Further it is unclear whether responses to DDR1 inhibition will be limited to those tumors that present with extensive stromal deposition or, as suggested by *in vitro* data with AsPC-1 cells, autocrine stimulation is critical to DDR1 activation on tumor cells. Addressing these questions is now feasible with the development of highly selective DDR1 inhibitors such as 7rh.

Supplementary Material

Refer to Web version on PubMed Central for supplementary material.

Acknowledgments

Grant support

This work is supported in part by the NIH (R01CA118240 and U54 CA210181 Project 2 to RAB; F31 CA168350 to KYA), CPRIT (RP160211 to DHC), the National Science Fund for Distinguished Young Scholars (#81425021 to KD), the 100 Distinguished Scientist Award of Guangdong province (Nanyue-Baijie award to KD), Guangdong province (grant #2016A050502041 to XR), and the Effie Marie Cain Scholarship for Angiogenesis Research (RAB).

We gratefully acknowledge Dr. Miao Wang for *KPC* animal tissue, Dr. Hoon Hur for surgical assistance with the orthotopic implantation of Pan02 cells, Dr. Lisa Li for assistance in therapeutic dosing of animals, Dr. James Kim for helpful comments on the manuscript and Dave Primm for editorial assistance.

References

1. Provenzano PP, Inman DR, Eliceiri KW, Knittel JG, Yan L, Rueden CT, et al. Collagen density promotes mammary tumor initiation and progression. BMC medicine. 2008; 6:11.doi: 10.1186/1741-7015-6-11 [PubMed: 18442412]
2. Conklin MW, Keely PJ. Why the stroma matters in breast cancer: insights into breast cancer patient outcomes through the examination of stromal biomarkers. Cell adhesion & migration. 2012; 6(3): 249–60. DOI: 10.4161/cam.20567 [PubMed: 22568982]
3. Mahadevan D, Von Hoff DD. Tumor-stroma interactions in pancreatic ductal adenocarcinoma. Mol Cancer Ther. 2007; 6(4):1186–97. doi 1535-7163.MCT-06-0686 [pii] 10.1158/1535-7163.MCT-06-0686. [PubMed: 17406031]
4. Liu H, Ma Q, Xu Q, Lei J, Li X, Wang Z, et al. Therapeutic potential of perineural invasion, hypoxia and desmoplasia in pancreatic cancer. Current pharmaceutical design. 2012; 18(17):2395–403. [PubMed: 22372500]
5. Vogel W, Gish GD, Alves F, Pawson T. The discoidin domain receptor tyrosine kinases are activated by collagen. Mol Cell. 1997; 1(1):13–23. doi S1097-2765(00)80003-9 [pii]. [PubMed: 9659899]
6. Shrivastava A, Radziejewski C, Campbell E, Kovac L, McGlynn M, Ryan TE, et al. An orphan receptor tyrosine kinase family whose members serve as nonintegrin collagen receptors. Mol Cell. 1997; 1(1):25–34. [PubMed: 9659900]
7. Kadler KE, Baldock C, Bella J, Boot-Handford RP. Collagens at a glance. Journal of Cell Science. 2007; 120(12):1955–8. DOI: 10.1242/Jcs.03453 [PubMed: 17550969]
8. Couvelard A, Hu J, Steers G, O'Toole D, Sauvanet A, Belghiti J, et al. Identification of potential therapeutic targets by gene-expression profiling in pancreatic endocrine tumors. Gastroenterology. 2006; 131(5):1597–610. DOI: 10.1053/j.gastro.2006.09.007 [PubMed: 17064702]
9. Johnson JD, Edman JC, Rutter WJ. A receptor tyrosine kinase found in breast carcinoma cells has an extracellular discoidin I-like domain. Proc Natl Acad Sci U S A. 1993; 90(12):5677–81. [PubMed: 8390675]
10. Laval S, Butler R, Shelling AN, Hanby AM, Poulsom R, Ganesan TS. Isolation and characterization of an epithelial-specific receptor tyrosine kinase from an ovarian cancer cell line. Cell growth & differentiation : the molecular biology journal of the American Association for Cancer Research. 1994; 5(11):1173–83. [PubMed: 7848919]
11. Perez JL, Shen X, Finkernagel S, Sciorra L, Jenkins NA, Gilbert DJ, et al. Identification and chromosomal mapping of a receptor tyrosine kinase with a putative phospholipid binding sequence in its ectodomain. Oncogene. 1994; 9(1):211–9. [PubMed: 8302582]
12. Karn T, Holtrich U, Brauninger A, Bohme B, Wolf G, Rubsamen-Waigmann H, et al. Structure, expression and chromosomal mapping of TKT from man and mouse: a new subclass of receptor tyrosine kinases with a factor VIII-like domain. Oncogene. 1993; 8(12):3433–40. [PubMed: 8247548]
13. Lai C, Lemke G. Structure and expression of the Tyro 10 receptor tyrosine kinase. Oncogene. 1994; 9(3):877–83. [PubMed: 8108131]
14. Alves F, Vogel W, Mossie K, Millauer B, Hofler H, Ullrich A. Distinct structural characteristics of discoidin I subfamily receptor tyrosine kinases and complementary expression in human cancer. Oncogene. 1995; 10(3):609–18. [PubMed: 7845687]
15. Alves F. Identification of two novel, kinase-deficient variants of discoidin domain receptor 1: differential expression in human colon cancer cell lines. The FASEB Journal. 2001; doi: 10.1096/fj.00-0626fje
16. Valiathan RR, Marco M, Leitinger B, Kleer CG, Fridman R. Discoidin domain receptor tyrosine kinases: new players in cancer progression. Cancer Metastasis Rev. 2012; 31(1–2):295–321. DOI: 10.1007/s10555-012-9346-z [PubMed: 22366781]

17. Leitinger B. Discoidin domain receptor functions in physiological and pathological conditions. International review of cell and molecular biology. 2014; 310:39–87. DOI: 10.1016/B978-0-12-800180-6.00002-5 [PubMed: 24725424]

18. Kalluri R, Zeisberg M. Fibroblasts in cancer. Nat Rev Cancer. 2006; 6(5):392–401. DOI: 10.1038/nrc1877 [PubMed: 16572188]

19. Apte MV, Park S, Phillips PA, Santucci N, Goldstein D, Kumar RK, et al. Desmoplastic reaction in pancreatic cancer: role of pancreatic stellate cells. Pancreas. 2004; 29(3):179–87. [PubMed: 15367883]

20. Cader FZ, Vockerodt M, Bose S, Nagy E, Brundler MA, Kearns P, et al. The EBV oncogene LMP1 protects lymphoma cells from cell death through the collagen-mediated activation of DDR1. Blood. 2013; 122(26):4237–45. DOI: 10.1182/blood-2013-04-499004 [PubMed: 24136166]

21. Ongusaha PP, Kim JI, Fang L, Wong TW, Yancopoulos GD, Aaronson SA, et al. p53 induction and activation of DDR1 kinase counteract p53-mediated apoptosis and influence p53 regulation through a positive feedback loop. EMBO J. 2003; 22(6):1289–301. DOI: 10.1093/emboj/cdg129 [PubMed: 12628922]

22. Jian ZX, Sun J, Chen W, Jin HS, Zheng JH, Wu YL. Involvement of discoidin domain 1 receptor in recurrence of hepatocellular carcinoma by genome-wide analysis. Medical oncology. 2012; 29(5):3077–82. DOI: 10.1007/s12032-012-0277-x [PubMed: 22752569]

23. Shintani Y, Fukumoto Y, Chaika N, Svoboda R, Wheelock MJ, Johnson KR. Collagen I-mediated up-regulation of N-cadherin requires cooperative signals from integrins and discoidin domain receptor 1. J Cell Biol. 2008; 180(6):1277–89. doi jcb.200708137 [pii] 10.1083/jcb.200708137. [PubMed: 18362184]

24. Park HS, Kim KR, Lee HJ, Choi HN, Kim DK, Kim BT, et al. Overexpression of discoidin domain receptor 1 increases the migration and invasion of hepatocellular carcinoma cells in association with matrix metalloproteinase. Oncol Rep. 2007; 18(6):1435–41. [PubMed: 17982627]

25. Kim HG, Hwang SY, Aaronson SA, Mandinova A, Lee SW. DDR1 receptor tyrosine kinase promotes prosurvival pathway through Notch1 activation. J Biol Chem. 2011; 286(20):17672–81. DOI: 10.1074/jbc.M111.236612 [PubMed: 21398698]

26. Ford CE, Lau SK, Zhu CQ, Andersson T, Tsao MS, Vogel WF. Expression and mutation analysis of the discoidin domain receptors 1 and 2 in non-small cell lung carcinoma. Br J Cancer. 2007; 96(5):808–14. DOI: 10.1038/sj.bjc.6603614 [PubMed: 17299390]

27. Miao L, Zhu S, Wang Y, Li Y, Ding J, Dai J, et al. Discoidin domain receptor 1 is associated with poor prognosis of non-small cell lung cancer and promotes cell invasion via epithelial-to-mesenchymal transition. Medical oncology. 2013; 30(3):626.doi: 10.1007/s12032-013-0626-4 [PubMed: 23761027]

28. Gao M, Duan L, Luo J, Zhang L, Lu X, Zhang Y, et al. Discovery and optimization of 3-(2-(Pyrazolo[1,5-a]pyrimidin-6-yl)ethynyl)benzamides as novel selective and orally bioavailable discoidin domain receptor 1 (DDR1) inhibitors. J Med Chem. 2013; 56(8):3281–95. DOI: 10.1021/jm301824k [PubMed: 23521020]

29. Ali-Rahmani F, FitzGerald DJ, Martin S, Patel P, Prunotto M, Ormanoglu P, et al. Anticancer Effects of Mesothelin-Targeted Immunotoxin Therapy Are Regulated by Tyrosine Kinase DDR1. Cancer Res. 2016; 76(6):1560–8. DOI: 10.1158/0008-5472.CAN-15-2401 [PubMed: 26719540]

30. Ambrogio C, Gomez-Lopez G, Falcone M, Vidal A, Nadal E, Crosetto N, et al. Combined inhibition of DDR1 and Notch signaling is a therapeutic strategy for KRAS-driven lung adenocarcinoma. Nat Med. 2016; 22(3):270–7. DOI: 10.1038/nm.4041 [PubMed: 26855149]

31. Hur H, Ham IH, Lee D, Jin H, Aguilera KY, Oh HJ, et al. Discoidin domain receptor 1 activity drives an aggressive phenotype in gastric carcinoma. BMC Cancer. 2017; 17(1):87.doi: 10.1186/s12885-017-3051-9 [PubMed: 28143619]

32. Wang M, Topalovski M, Toombs JE, Wright CM, Moore ZR, Boothman DA, et al. Fibulin-5 Blocks Microenvironmental ROS in Pancreatic Cancer. Cancer Res. 2015; 75(23):5058–69. DOI: 10.1158/0008-5472.CAN-15-0744 [PubMed: 26577699]

33. Beck AW, Luster TA, Miller AF, Holloway SE, Conner CR, Barnett CC, et al. Combination of a monoclonal anti-phosphatidylserine antibody with gemcitabine strongly inhibits the growth and

metastasis of orthotopic pancreatic tumors in mice. Int J Cancer. 2006; 118(10):2639–43. DOI: 10.1002/ijc.21684 [PubMed: 16353142]

34. Arnold S, Mira E, Muneer S, Korpanty G, Beck AW, Holloway SE, et al. Forced expression of MMP9 rescues the loss of angiogenesis and abrogates metastasis of pancreatic tumors triggered by the absence of host SPARC. Exp Biol Med (Maywood). 2008; 233(7):860–73. doi 0801-RM-12 [pii] 10.3181/0801-RM-12. [PubMed: 18445772]
35. Hingorani SR, Wang L, Multani AS, Combs C, Deramaudt TB, Hruban RH, et al. Trp53R172H and KrasG12D cooperate to promote chromosomal instability and widely metastatic pancreatic ductal adenocarcinoma in mice. Cancer Cell. 2005; 7(5):469–83. doi S1535-6108(05)00128-5 [pii] 10.1016/j.ccr.2005.04.023. [PubMed: 15894267]
36. Seymour PA, Freude KK, Dubois CL, Shih HP, Patel NA, Sander M. A dosage-dependent requirement for Sox9 in pancreatic endocrine cell formation. Developmental biology. 2008; 323(1):19–30. DOI: 10.1016/j.ydbio.2008.07.034 [PubMed: 18723011]
37. Furuyama K, Kawaguchi Y, Akiyama H, Horiguchi M, Kodama S, Kuhara T, et al. Continuous cell supply from a Sox9-expressing progenitor zone in adult liver, exocrine pancreas and intestine. Nat Genet. 2011; 43(1):34–41. DOI: 10.1038/ng.722 [PubMed: 21113154]
38. Mihai C, Chotani M, Elton TS, Agarwal G. Mapping of DDR1 distribution and oligomerization on the cell surface by FRET microscopy. J Mol Biol. 2009; 385(2):432–45. DOI: 10.1016/j.jmb.2008.10.067 [PubMed: 19007791]
39. Chauhan VP, Martin JD, Liu H, Lacorre DA, Jain SR, Kozin SV, et al. Angiotensin inhibition enhances drug delivery and potentiates chemotherapy by decompressing tumour blood vessels. Nat Commun. 2013; 4:2516.doi: 10.1038/ncomms3516 [PubMed: 24084631]
40. Huang H, Svoboda RA, Lazenby AJ, Saowapa J, Chaika N, Ding K, et al. Up-regulation of N-cadherin by Collagen I-activated Discoidin Domain Receptor 1 in Pancreatic Cancer Requires the Adaptor Molecule Shc1. J Biol Chem. 2016; 291(44):23208–23. DOI: 10.1074/jbc.M116.740605 [PubMed: 27605668]
41. Li X, Ma Q, Xu Q, Duan W, Lei J, Wu E. Targeting the cancer-stroma interaction: a potential approach for pancreatic cancer treatment. Current pharmaceutical design. 2012; 18(17):2404–15. [PubMed: 22372501]
42. Aguilera KY, Rivera LB, Hur H, Carbon JG, Toombs JE, Goldstein CD, et al. Collagen signaling enhances tumor progression after anti-VEGF therapy in a murine model of pancreatic ductal adenocarcinoma. Cancer Res. 2014; 74(4):1032–44. DOI: 10.1158/0008-5472.CAN-13-2800 [PubMed: 24346431]
43. Sato N, Fukushima N, Maehara N, Matsubayashi H, Koopmann J, Su GH, et al. SPARC/osteonectin is a frequent target for aberrant methylation in pancreatic adenocarcinoma and a mediator of tumor-stromal interactions. Oncogene. 2003; 22(32):5021–30. doi 10.1038/sj.onc.1206807 1206807 [pii]. [PubMed: 12902985]
44. Cheetham S, Tang MJ, Mesak F, Kennecke H, Owen D, Tai IT. SPARC promoter hypermethylation in colorectal cancers can be reversed by 5-Aza-2'deoxycytidine to increase SPARC expression and improve therapy response. Br J Cancer. 2008; 98(11):1810–9. DOI: 10.1038/sj.bjc.6604377 [PubMed: 18458674]
45. Tai IT, Dai M, Owen DA, Chen LB. Genome-wide expression analysis of therapy-resistant tumors reveals SPARC as a novel target for cancer therapy. J Clin Invest. 2005; 115(6):1492–502. DOI: 10.1172/JCI23002 [PubMed: 15902309]
46. Von Hoff DD, Ramanathan RK, Borad MJ, Laheru DA, Smith LS, Wood TE, et al. Gemcitabine plus nab-paclitaxel is an active regimen in patients with advanced pancreatic cancer: a phase I/II trial. J Clin Oncol. 2011; 29(34):4548–54. doi JCO.2011.36.5742 [pii] 10.1200/JCO.2011.36.5742. [PubMed: 21969517]
47. Lindner JL, Loibl S, Denkert C, Ataseven B, Fasching PA, Pfitzner BM, et al. Expression of secreted protein acidic and rich in cysteine (SPARC) in breast cancer and response to neoadjuvant chemotherapy. Annals of oncology : official journal of the European Society for Medical Oncology / ESMO. 2015; 26(1):95–100. DOI: 10.1093/annonc/mdu487
48. Erkan M, Michalski CW, Rieder S, Reiser-Erkan C, Abiatari I, Kolb A, et al. The activated stroma index is a novel and independent prognostic marker in pancreatic ductal adenocarcinoma. Clin

Gastroenterol Hepatol. 2008; 6(10):1155–61. doi S1542-3565(08)00498-9 [pii] 10.1016/j.cgh.2008.05.006. [PubMed: 18639493]

49. Das S, Ongusaha PP, Yang YS, Park JM, Aaronson SA, Lee SW. Discoidin domain receptor 1 receptor tyrosine kinase induces cyclooxygenase-2 and promotes chemoresistance through nuclear factor-kappaB pathway activation. Cancer Res. 2006; 66(16):8123–30. DOI: 10.1158/0008-5472.CAN-06-1215 [PubMed: 16912190]
50. Kerroch M, Guerrot D, Vandermeersch S, Placier S, Mesnard L, Jouanneau C, et al. Genetic inhibition of discoidin domain receptor 1 protects mice against crescentic glomerulonephritis. FASEB J. 2012; 26(10):4079–91. DOI: 10.1096/fj.11-194902 [PubMed: 22751008]
51. Valencia K, Ormazabal C, Zandueta C, Luis-Ravelo D, Anton I, Pajares MJ, et al. Inhibition of collagen receptor discoidin domain receptor-1 (DDR1) reduces cell survival, homing, and colonization in lung cancer bone metastasis. Clin Cancer Res. 2012; 18(4):969–80. DOI: 10.1158/1078-0432.CCR-11-1686 [PubMed: 22223527]
52. Li Y, Lu X, Ren X, Ding K. Small Molecule Discoidin Domain Receptor Kinase Inhibitors and Potential Medical Applications. J Med Chem. 2015; doi: 10.1021/jm5012319
53. Day E, Waters B, Spiegel K, Alnadaf T, Manley PW, Buchdunger E, et al. Inhibition of collagen-induced discoidin domain receptor 1 and 2 activation by imatinib, nilotinib and dasatinib. Eur J Pharmacol. 2008; 599(1–3):44–53. doi S0014-2999(08)01025-X [pii] 10.1016/j.ejphar.2008.10.014. [PubMed: 18938156]
54. Rix U, Hantschel O, Durnberger G, Remsing Rix LL, Planyavsky M, Fernbach NV, et al. Chemical proteomic profiles of the BCR-ABL inhibitors imatinib, nilotinib, and dasatinib reveal novel kinase and nonkinase targets. Blood. 2007; 110(12):4055–63. DOI: 10.1182/blood-2007-07-102061 [PubMed: 17720881]
55. Maass N, Schem C, Bauerschlag DO, Tiemann K, Schaefer FW, Hanson S, et al. Final safety and efficacy analysis of a phase I/II trial with imatinib and vinorelbine for patients with metastatic breast cancer. Oncology. 2014; 87(5):300–10. DOI: 10.1159/000365553 [PubMed: 25171229]
56. Roskoski R Jr. Src protein-tyrosine kinase structure, mechanism, and small molecule inhibitors. Pharmacological research : the official journal of the Italian Pharmacological Society. 2015; 94:9–25. DOI: 10.1016/j.phrs.2015.01.003
57. Ding L, Getz G, Wheeler DA, Mardis ER, McLellan MD, Cibulskis K, et al. Somatic mutations affect key pathways in lung adenocarcinoma. Nature. 2008; 455(7216):1069–75. DOI: 10.1038/nature07423 [PubMed: 18948947]
58. Pitini V, Arrigo C, Di Mirto C, Mondello P, Altavilla G. Response to dasatinib in a patient with SQCC of the lung harboring a discoid-receptor-2 and synchronous chronic myelogenous leukemia. Lung Cancer. 2013; 82(1):171–2. DOI: 10.1016/j.lungcan.2013.07.004 [PubMed: 23932362]

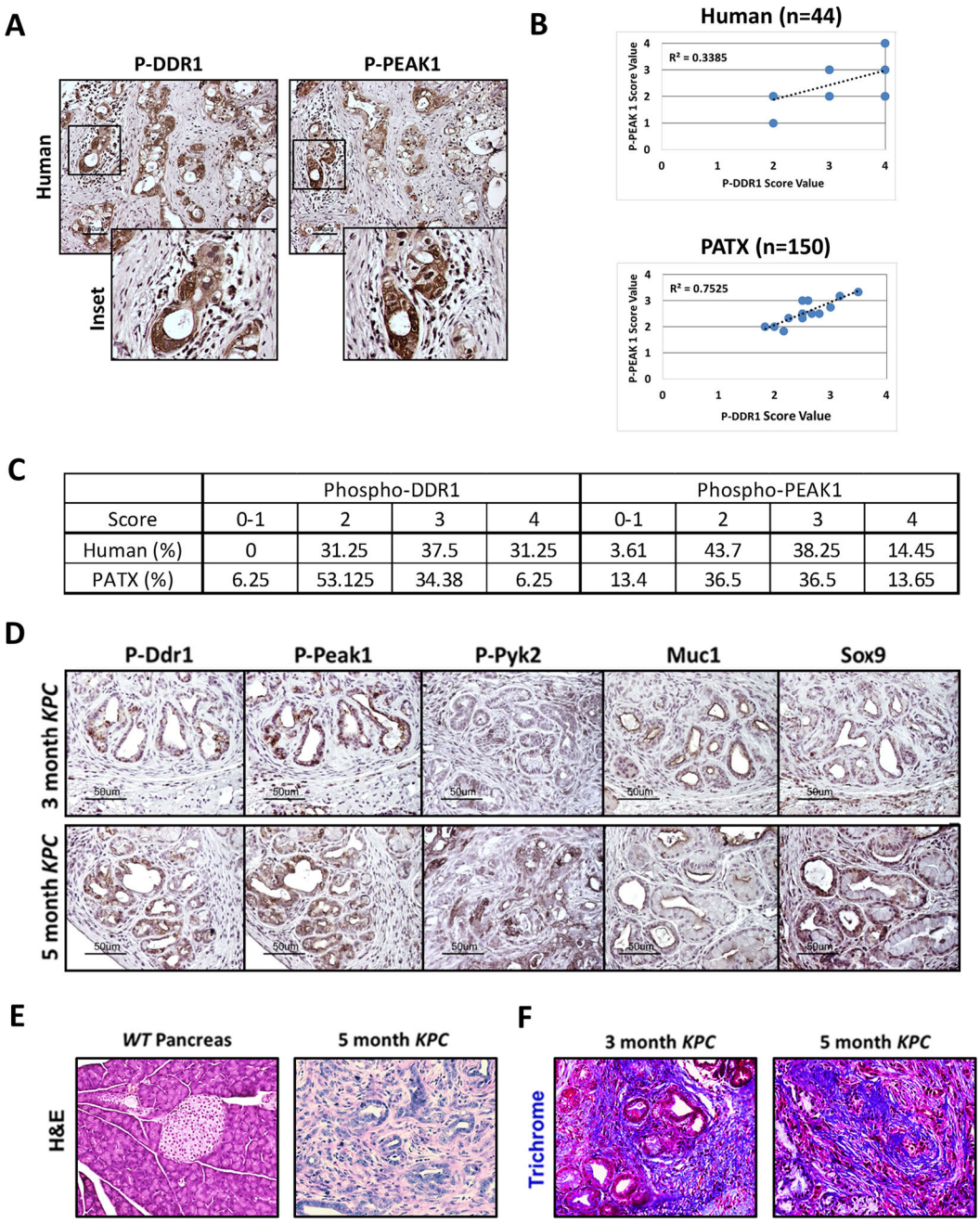

Figure 1. DDR1 signaling in human and mouse PDA

(A) Immunohistochemical detection of phospho-DDR1 and phospho-PEAK1 in human PDA. TMAs of primary human PDA (44 samples) demonstrated phospho-DDR1 and phospho-PEAK1 localized to similar regions. (B) Pearson correlation of p-PEAK1 and p-DDR1 expression in human and patient-derived tumor xenograft (PATX) TMA samples. (C) Percent of TMA samples positive for p-DDR1 and p-PEAK1. Scoring system is denoted as: low or no reactivity (0–1), moderate reactivity (2), strong reactivity (3), and very strong reactivity (4). (D–F) Histological analyses of the *KPC (LSL-Kras$^{G12D/+}$; LSL-Trp53$^{R172H/+}$; p48$^{Cre/+}$)* GEMM of PDA. (D) Immunohistochemical detection of phospho-Ddr1, phospho-

Peak1, phospho-Pyk2, Muc1, and Sox9 in *KPC* tumors. Ddr1 activation and downstream signaling through effectors such as Peak1 and Pyk2 was present in early PanIN lesions (similar to regions positive for Muc-1 staining) and in advanced adenocarcinoma (similar to regions of Sox9 staining). Tissue from an early (3-month) and advanced (5-month) stage of the *KPC* model was evaluated. (E) H&E histology of normal WT pancreas and PDA in a 5-month-old *KPC* mouse. (F) Trichrome analysis of PDA from 3- and 5-month-old *KPC* animals.

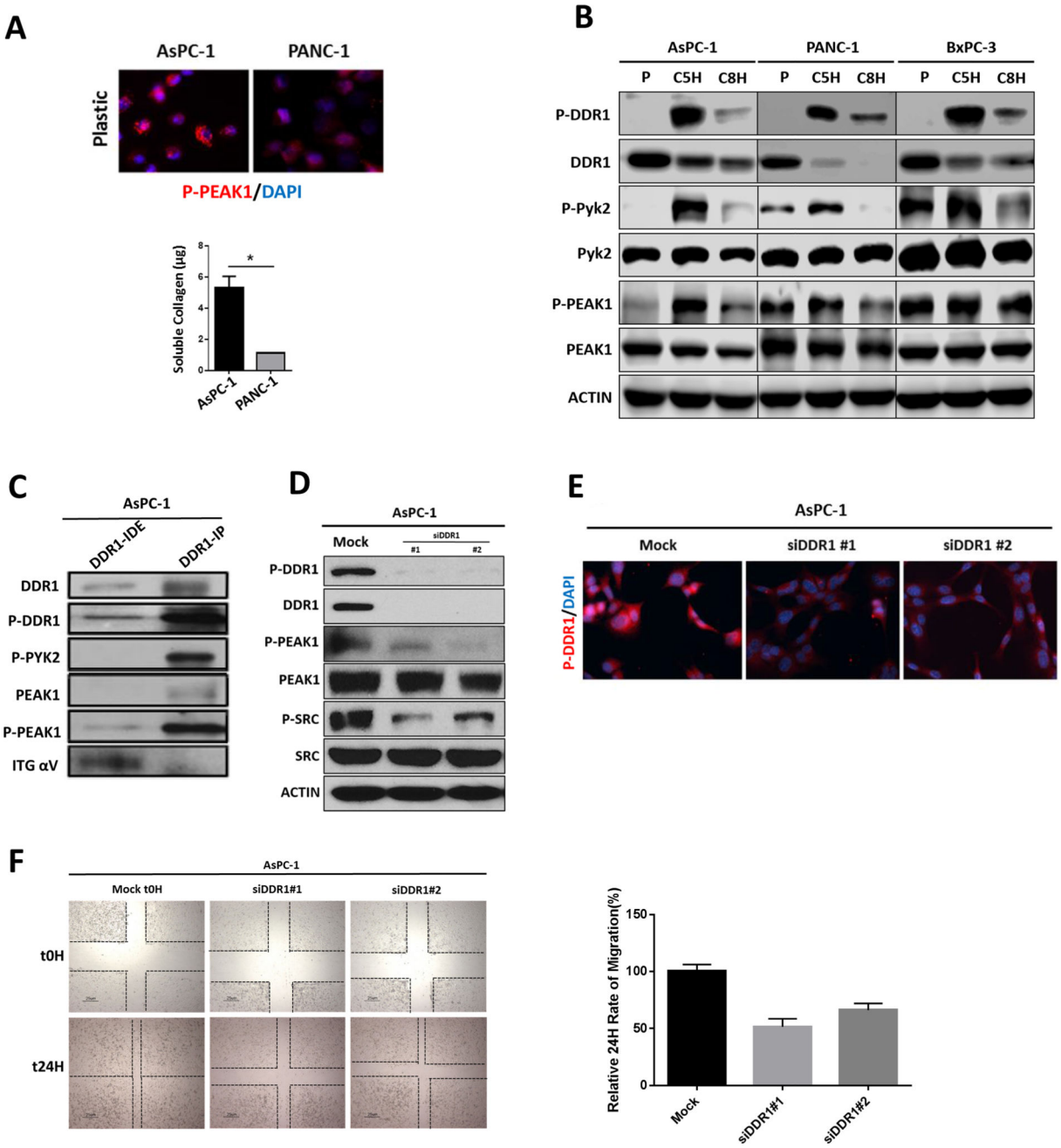

Figure 2. Effectors of DDR1 signaling in human PDA cell lines

(A) Human PDA cell lines were plated in the absence of collagen I. The phosphorylation of PEAK1 was detected by immunocytochemistry. The secretion of soluble collagen (µg) was assessed in duplicate samples of human PDA cells by Sircol analysis. This depicted that AsPC-1 secreted an elevated level of collagen compared to PANC-1 cells. (B) Human PDA cell lines AsPC-1, PANC-1 and BxPC-3 were plated on plastic (P) and stimulated with soluble collagen I (50 µg/ml) for 5 hours (C5H) or 8 hours (C8H). Lysates were probed for indicated targets by Western blot analysis. (C) Immunoprecipitation (IP) analysis of DDR1 interactions. The DDR1 IP pulled down PYK2 and PEAK1, but did not pull down alpha V

integrin (ITG αV) as shown in the immunodepleted (IDE) fraction. (D) siRNA-mediated knockdown of DDR1 compared to mock siRNA control reduced the activation of DDR1, PEAK1, and SRC. Lysates were probed for the indicated targets by Western blot analysis. (E) siRNA-mediated knockdown of DDR1 compared to mock siRNA control reduced the activation of DDR1 through immunocytochemistry. (F) siRNA-mediated knockdown of DDR1 compared to mock siRNA control reduced the migration of human PDA cells (AsPC-1) after a 24-hour period of time via scratch migration assay. Error bars: *, $p < 0.05$, one-way ANOVA with Tukey's MCT.

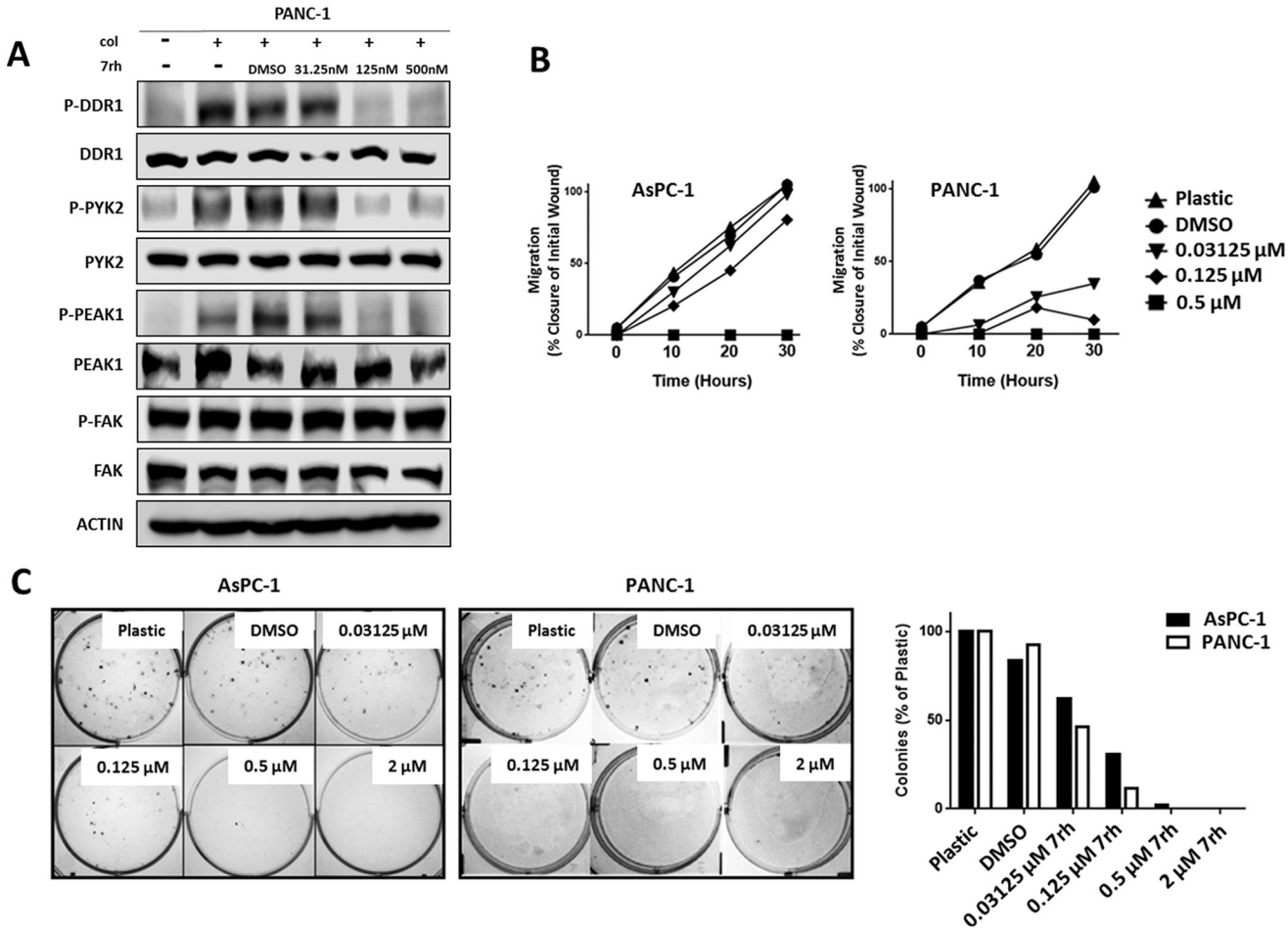

Figure 3. Signaling and functional consequences of DDR1 inhibition by 7rh in human PDA cell lines

(A) 7rh inhibited DDR1-mediated signaling in a concentration-dependent manner in human PDA cell line PANC-1. Lysates were probed for the indicated targets by Western blot analysis. (B) 7rh inhibited the migration of human PDA cell lines in a concentration-dependent manner over a 30-hour time period via scratch migration assay. (C) 7rh inhibited liquid colony formation of human PDA cell lines in a concentration-dependent manner.

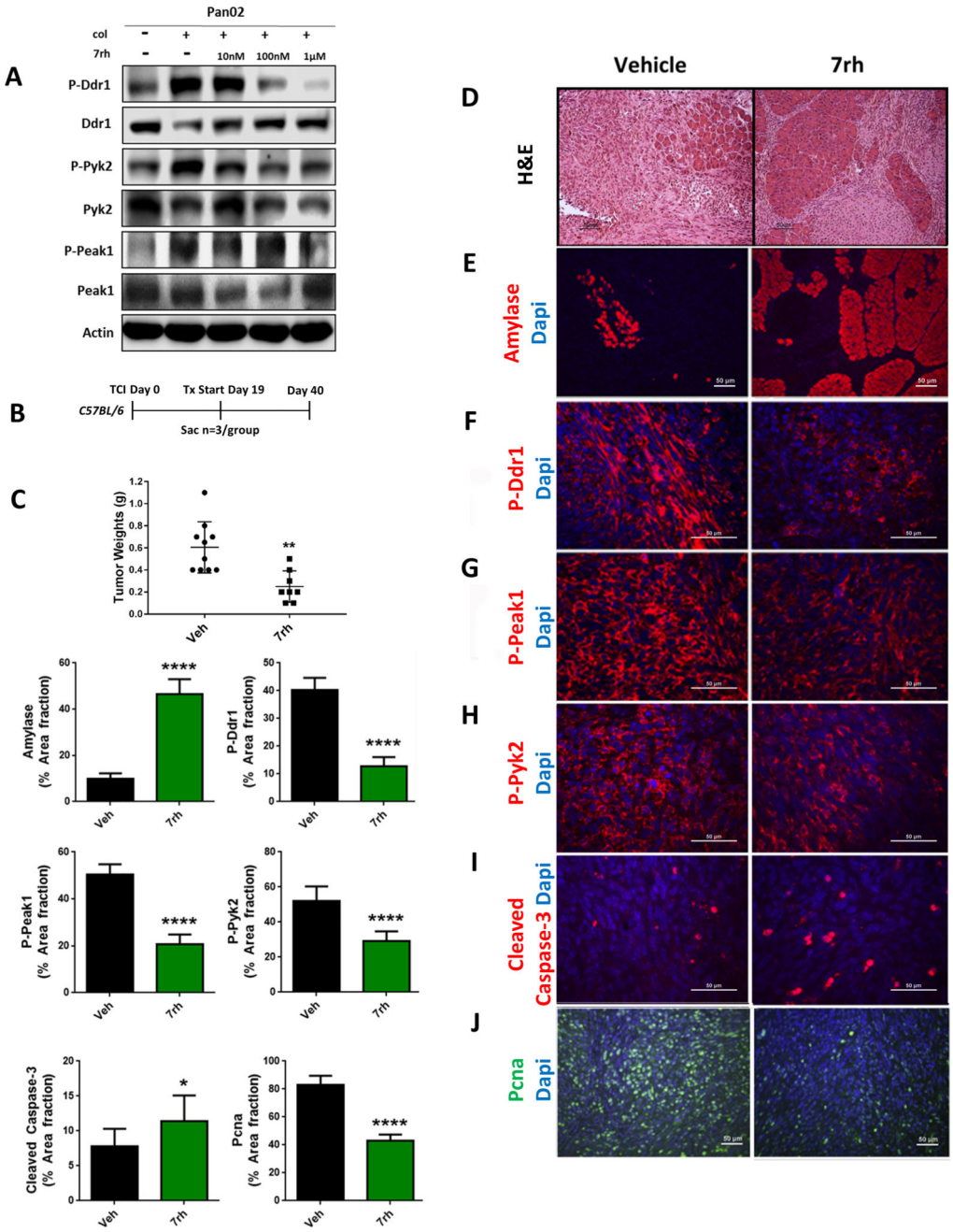

Figure 4. 7rh reduced Ddr1-mediated tumorigenicity and signaling

(A) 7rh inhibited DDR1-mediated signaling in a concentration-dependent manner in murine PDA cell line Pan02. Lysates were probed for the indicated targets by Western blot analysis. (B) Schematic representation of the animal experiment. Mouse Pan02 cell line was orthotopically injected into *C57BL/6* mice and 7rh therapy of 25 mg/kg 3×/week started at day 19 and ended at day 40. (C) 7rh treatment reduced tumor burden compared to vehicle and led to a greater presence of normal acinar tissue (D, E). (F–H) Immunohistochemical analysis of tissue from each group depicted inhibition of Ddr1 activation and downstream signaling (P-Peak1, P-Pyk2), as well as enhanced cellular apoptosis (I) and reduced

proliferation (J). Error bars: (*, $p < 0.05$; **, $p < 0.005$; ***, $p < 0.0005$; ****, $p < 0.00005$), one-way ANOVA with Tukey's MCT.

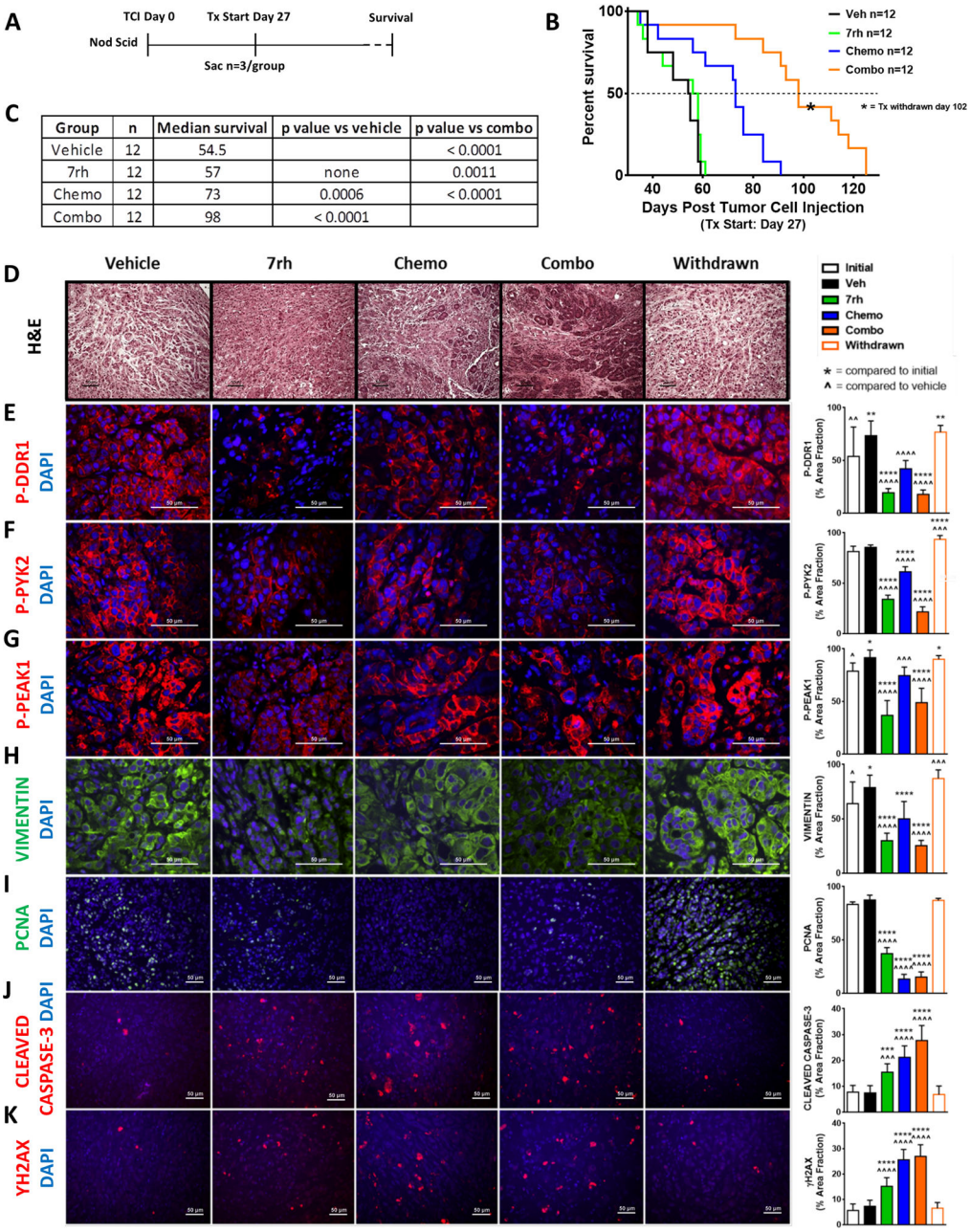

Figure 5. 7rh in combination with chemotherapy reduced DDR1-mediated signaling and tumorigenicity in a PDA xenograft model

(A) Schematic representation of the animal experiment. (B–C) 7rh combined with a chemotherapy regimen (gemcitabine + nab-paclitaxel) enhanced the overall median of survival in a xenograft PDA model of human cell line AsPC-1. (D–K) Immunohistological analysis of PDA tumors demonstrated that 7rh, chemotherapy, and the combination regimen enhanced the presence of a more normal pancreatic landscape (H&E), significantly inhibited DDR1-mediated signaling, and significantly reduced the levels of the mesenchymal marker VIMENTIN and proliferation (PCNA), and enhanced the levels of apoptosis (CLEAVED CASPASE-3) and DNA damage (ϒH2AX). Error bars: (*, $p < 0.05$; **, $p < 0.005$; ***, $p <$

0.0005; ****, $p < 0.00005$) compared to the initial group; (^, $p < 0.05$; ^^, $p < 0.005$; ^^^, $p < 0.0005$; ^^^^, $p < 0.00005$) compared to the vehicle group, one-way ANOVA with Tukey's MCT.

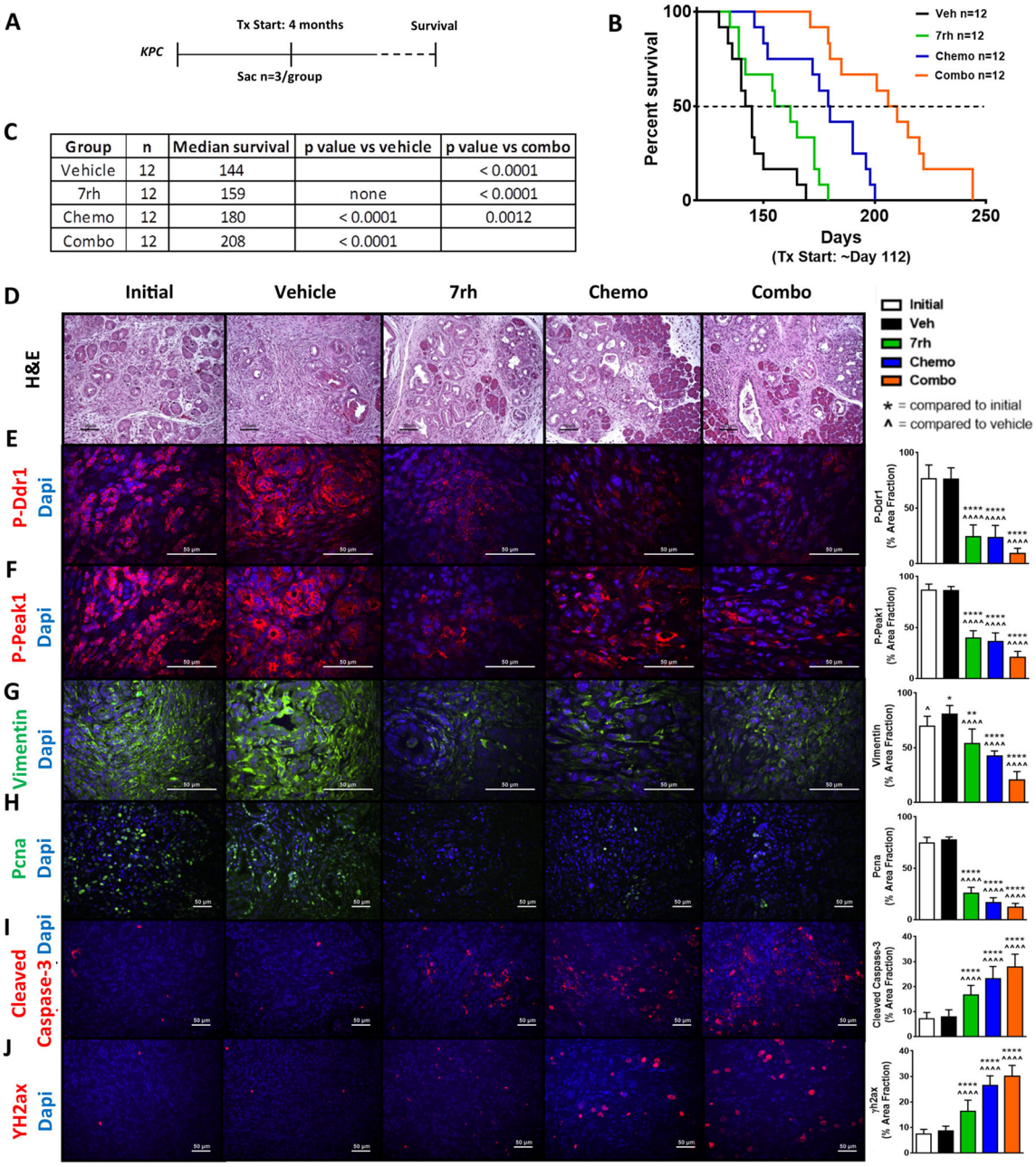

Group	n	Median survival	p value vs vehicle	p value vs combo
Vehicle	12	144		< 0.0001
7rh	12	159	none	< 0.0001
Chemo	12	180	< 0.0001	0.0012
Combo	12	208	< 0.0001	

Figure 6. 7rh in combination with chemotherapy reduced Ddr1-mediated signaling and tumorigenicity in a GEMM of PDA

(A) Schematic representation of the animal experiment. (B–C) 7rh combined with a chemotherapy regimen (gemcitabine + nab-paclitaxel) enhanced the overall median of survival in the *KPC* GEMM of PDA. (D–J) Immunohistological analyses of PDA tumors demonstrated that 7rh, chemotherapy, and the combination regimen significantly inhibited Ddr1-mediated signaling, the levels of the mesenchymal marker Vimentin and proliferation (Pcna) and induced apoptosis (Cleaved Caspase-3) and DNA damage (YH2ax). Error bars: (*, $p < 0.05$; **, $p < 0.005$; ***, $p < 0.0005$; ****, $p < 0.00005$) compared to the initial

group; (^, $p < 0.05$; ^^, $p < 0.005$; ^^^, $p < 0.0005$; ^^^^, $p < 0.00005$) compared to the vehicle group, one-way ANOVA with Tukey's MCT.

Table 1

Description of animal experiments

Endpoint:	Experiment start	10 days post tumor cell injection
	Animals	*C57BL*/6, (n = 3/group)
	Treatment groups	Vehicle: 1 dose
		7rh: 0.1 mg/kg, 1 dose
		7rh: 1 mg/kg, 1 dose
		7rh: 10 mg/kg, 1 dose
	Associated figures	Supplementary Figure 1
Endpoint:	Experiment start	10 days post tumor cell injection
7rh titration	Experiment length	21 days post tumor cell injection
	Animals	*C57BL*/6, (n = 5/group)
	Treatment groups	Vehicle: 3×/week
		7rh: 3.3 mg/kg, 3×/week
		7rh: 10 mg/kg, 3×/week
		7rh: 30 mg/kg, 3×/week
	Associated figures	Supplementary Figures 2–3
Endpoint:	Experiment start	19 days post tumor cell injection
7rh monotherapy	Experiment length	40 days post tumor cell injection
	Animals	*C57BL/6,* (n = 16/group)
	Treatment groups	Vehicle: 3×/week
		7rh: 25 mg/kg, 3×/week
	Associated figures	Figure 4
Survival:	Experiment start	27 days post tumor cell injection
7rh +/− chemo	Experiment length	Until moribund
	Animals	Nod Scid, (n = 12/group)
	Treatment groups	Vehicle: 3×/week
		7rh: 25 mg/kg, 3×/week
		Chemotherapy: Gem (12.5 mg/kg, 2×/week), Nab-pac (5 mg/kg, 2×/week)
		Combination: 7rh + chemotherapy
	Associated figures	Figure 5, Supplementary Figure 4
Survival:	Experiment start	16 weeks old
7rh +/− chemo	Experiment length	Until moribund
	Animals	*KPC (LSL-Kras$^{G12D/+}$; LSL-Trp53$^{R172H/+}$; P48-Cre),* (n = 12/group)
	Treatment groups	Vehicle: 3×/week
		7rh: 25 mg/kg, 3×/week
		Chemotherapy: Gem (12.5 mg/kg, 2×/week), Nab-pac (5 mg/kg, 2×/week)
		Combination: 7rh + chemotherapy
	Associated figures	Figure 6, Supplementary Figure 5

Abbreviations: Gem, gemcitabine; Nab-pac, nab-paclitaxel.